Laterally confined metal-to-insulator and quasi-two-dimensional–to–two-dimensional transition by focused Rb intercalation of $1T$-TaS_2

D. J. Rahn,[1] E. Ludwig,[1] J. Buck,[1] F. Kronast,[2] M. Marczynski-Bühlow,[1] E. Kröger,[1] L. Kipp,[1] and K. Rossnagel[1]

[1]*Institut für Experimentelle und Angewandte Physik, Christian-Albrechts-Universität zu Kiel, D-24098 Kiel, Germany*

[2]*Helmholtz-Zentrum Berlin für Materialien und Energie, D-12489 Berlin, Germany*

(Received 14 November 2011; revised manuscript received 16 December 2011; published 28 December 2011)

Submicrometer lateral control of the surface electronic properties of the layered correlated electron material $1T$-TaS_2 is achieved *in situ* by focused Rb deposition at room temperature and verified using photoemission microscopy and spectroscopy, as well as scanning tunneling microscopy. The laterally confined Rb deposition results in the formation of a dense pattern of insulating islands in a metallic background. The local metal-to-insulator transitions are driven by Rb intercalation and accompanied by a change of the dimensionality of the surface electronic structure from quasi-2D to essentially 2D. The results establish the feasibility of spatially controlled *in situ* intercalation of layered materials.

DOI: 10.1103/PhysRevB.84.233105 PACS number(s): 71.30.+h, 73.22.−f, 79.60.−i

I. INTRODUCTION

Correlated electron materials are presently widely regarded as a basis for future electronics, mostly for three reasons.[1–3] First, these materials provide functionality not found in conventional semiconductors, including charge, spin, and orbital ordered phases, superconductivity, and metal-to-insulator transitions.[4–6] Second, they show extreme sensitivity to small perturbations when they are tuned to regimes where several different electronic phases are close in energy.[6] Third, they should in principle be downsizable to nanoscale dimensions without reaching the limits of carrier density fluctuations.[7]

While artificial oxide heterostructures are currently at the center of attention in "correlated electronics",[1–3] there are many naturally layered systems that may turn out to be useful as well. Here, we specifically focus on the intriguing correlated electron material $1T$-TaS_2, which belongs to the family of layered transition-metal dichalcogenides.[8] These compounds, consisting of van der Waals bonded chalcogen-transition metal-chalcogen sandwiches [see Fig. 1(b)], are well known for their diversity of charge-density-wave (CDW) phases[9,10] and the ability to store electron-donating atoms or molecules in the van der Waals gaps.[11] Pristine $1T$-TaS_2 specifically displays multiple structural changes associated with the formation of a $(\sqrt{13} \times \sqrt{13})$ CDW and undergoes a Mott-Hubbard-type metal-to-insulator transition well above liquid nitrogen temperatures.[12–14] Moreover, the material turns into a superconductor under hydrostatic pressure[15] and it enters several other CDW phases of different symmetries upon intercalation with alkali metals, Cu, or N_2H_4.[16–24] Particularly remarkable is an alkali intercalation-induced transformation into a $c(2\sqrt{3} \times 4)$ *rect*. CDW phase at room temperature that comes along with a distinct metal-to-insulator transition.[20–24]

Alkali intercalation is an especially interesting control parameter for the electronic properties of layered materials because it can be applied *in situ*,[25] and because it leads not only to electron doping of the host lattice[11] but also to an effective reduction of the dimensionality from quasi-2D to essentially 2D via an increase of the interlayer separation.[26] However, lateral control of alkali intercalation on submicrometer length scales, as would be required for nanoscale device application, has not yet been accomplished. Here we present a first step toward such a level of spatial control by implementing focused Rb deposition on $1T$-TaS_2. Employing scanning tunneling microscopy (STM), photoelectron emission microscopy (PEEM), and angle-resolved photoemission spectroscopy (ARPES), we specifically show that the Rb intercalation-induced metal-to-insulator and quasi-2D-to-2D transition in $1T$-TaS_2 can be sharply confined to nanoscale islands, and that larger structures consisting of a dense pattern of such islands can be written with micrometer precision.

II. METHODS

The single-crystal $1T$-TaS_2 samples used in the experiments reported here were grown via iodine vapor transport. Clean surfaces were prepared by cleavage in ultrahigh vacuum. Focused Rb deposition was achieved *in situ* using the home-built evaporator depicted in Fig. 1(a). The evaporator consists of a (carefully outgassed) SAES-Getters Rb dispenser and a 50 mm long, liquid-nitrogen-cooled collimator with a 2-mm entrance pinhole and a 5×0.3-mm^2 exit slit, placed less than 500 μm above the sample surface. In a typical deposition run, the evaporator current was set to 6 A for 3–20 min and the pressure stayed below 10^{-9} mbar. During all preparations and subsequent measurements, the samples were held at room temperature.

For STM measurements, a modified Omicron instrument was used. PEEM measurements were performed at beamline UE49-PGMa of BESSY II (Berlin) using an Elmitec system. Photoelectrons were imaged in normal-emission geometry at an energy resolution of 350 meV and an angular acceptance of $\pm 8^\circ$. Photon-energy dependent ARPES measurements were done at beamline BW3 of DORIS III (Hamburg) with a SPECS Phoibos 150 hemispherical electron analyzer, also in normal-emission geometry. Here, the energy and angular resolutions were $\sim$100 meV and 0.5°, respectively. The spatial resolutions

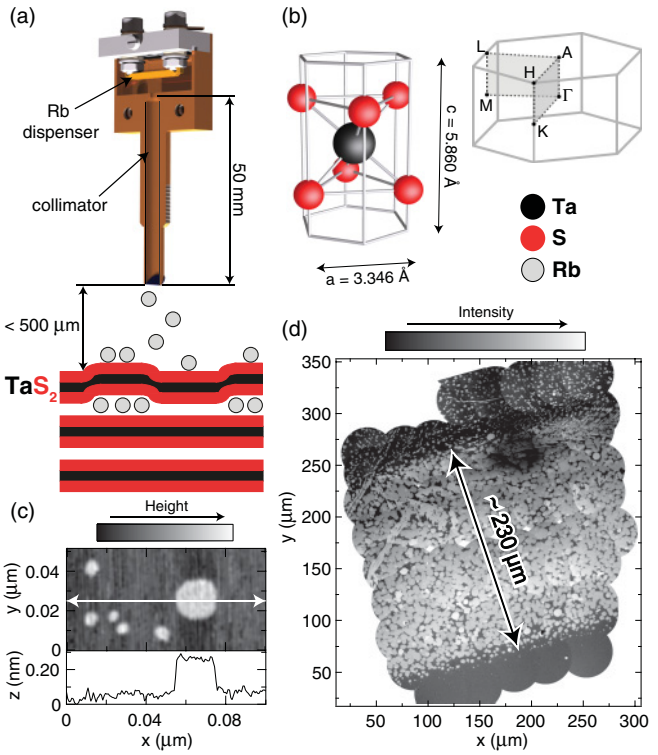

FIG. 1. (Color online) (a) Schematic illustration of the setup used for focused Rb deposition resulting in laterally confined intercalation of the layered compound $1T$-TaS_2. (b) Hexagonal unit cells of $1T$-TaS_2 in real space and momentum space. Lattice constants[8] and high-symmetry points are indicated. (c) Constant-current STM image and selected line scan taken after 3 min of unfocused Rb deposition (bias voltage: 0.5 V; tunneling current: 0.25 nA). (d) Overview PEEM image, composed of 84 individual images that were taken with a Hg vapor lamp after 6.5 min of focused Rb deposition ($h\nu = 4.9$ eV).

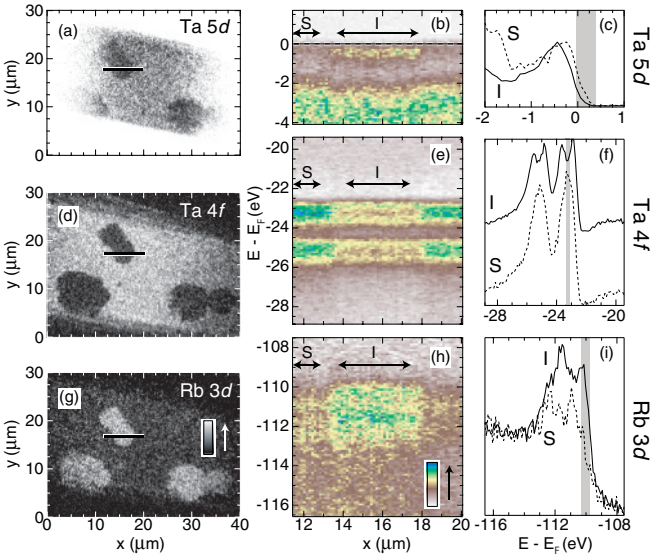

FIG. 2. (Color online) PEEM microspectroscopy of Rb/$1T$-TaS_2 (after 20 min of focused Rb deposition) at electron energies corresponding to emissions from (a)–(c) Ta $5d$ ($h\nu = 120$ eV), (d)–(f) Ta $4f$ ($h\nu = 170$ eV), and (g)–(i) Rb $3d$ states ($h\nu = 170$ eV). (a), (d), (g) Energy-resolved PEEM images integrated over the energy intervals marked by the gray bars in (c), (f), and (i). (b), (e), (h) PEEM spectra along the lines indicated in (a), (d), and (g). (c), (f), (i) PEEM spectra integrated over the regions denoted by "S" (surface Rb) and "I" (intercalated Rb) in (b), (e), and (h).

(FWHM) were 1.2 nm (STM), 250 nm (PEEM), and 250 μm (ARPES).

The results obtained under the described conditions were reproducible in the sense that for macroscopically faceted $1T$-TaS_2 surfaces, a high density of Rb intercalated regions [as in Fig. 1(d)] could typically be observed after a deposition time of 6.5 min. For flat and shiny surfaces, on the other hand, it took three to four times longer to reach the same state.

III. RESULTS AND DISCUSSION

Figure 1(d) shows a composite overview PEEM image taken with a Hg vapor lamp after focused Rb deposition on $1T$-TaS_2. The image directly reflects the variation of the work function on the surface (higher photoemission intensity corresponding to lower work function) and reveals a stripe of reduced work function whose width is slightly smaller than the exit slit width of the evaporator. The stripe is a dense arrangement of islands with typical sizes varying between 100 nm^2 and 100 μm^2 and covers about 82% of the surface. At the fringes of the stripe, however, the islands become smaller and their density decreases. In agreement with a previous STM study,[27] the STM image and the extracted height profile shown in Fig. 1(c) indicate that the formation of the islands is associated with an elevation of the sample surface of about 2 Å. Both observations (reduced work function and elevated surface) are consistent with Rb intercalation into the topmost van der Waals gap of the layered material, as schematically illustrated in Fig. 1(a).

The PEEM microspectroscopy results shown in Fig. 2 corroborate this interpretation. The images taken at specific valence-band and core-level energies (left column), the series of spectra scanned across a selected island (middle column), and the corresponding pairs of spectra recorded on and off the island (right column) display three characteristic spectroscopic signatures known from spatially integrated photoemission experiments on alkali-metal intercalated $1T$-TaX_2 (X = S, Se).[19–22,24,28,29] These are (i) the complete removal of Ta $5d$ spectral weight from the Fermi level indicating a distinct metal-to-insulator transition [Figs. 2(a)–2(c)], (ii) an increased splitting of the Ta $4f$ core levels due to a change of the symmetry of the CDW [Figs. 2(d)–2(f)], and (iii) the appearance of a new peak in the Rb $3d$ spectrum at higher energies (around $E - E_F = -110$ eV) serving as the most direct proof of Rb atoms having entered a chemical environment that is different from the one on the surface [Figs. 2(g)–2(i)]. Remarkably, all these spectral modifications are spatially well confined to islands of intercalated Rb, and they are perfectly spatially correlated within the precision of the experiment [see Figs. 2(a), 2(d), 2(g), 2(b), 2(e), and 2(h)]. The comparison of the photoemission intensities

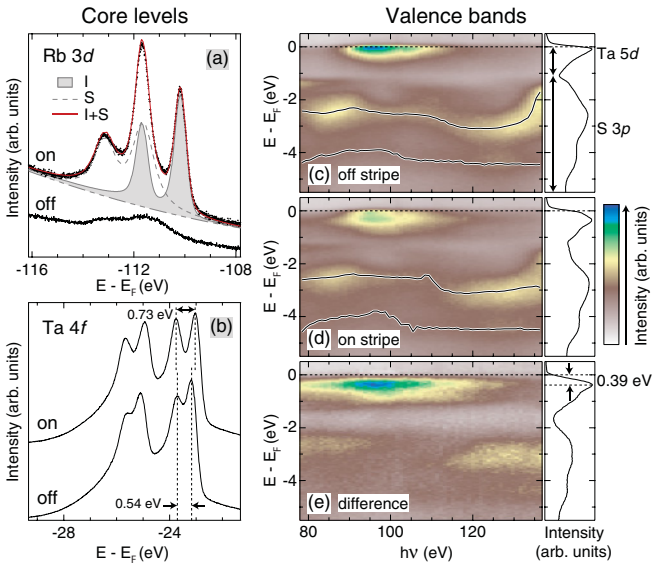

FIG. 3. (Color online) ARPES spectra of Rb/1T-TaS_2 taken on and off a stripe created by focused Rb deposition (for 6.5 min). (a) Rb 3d core-level spectra ($h\nu = 180$ eV). A decomposition of the spectrum recorded on the stripe into Doniach-Šunjić-type spectral lines corresponding to surface Rb ('S') and intercalated Rb ('I') is indicated. (b) Ta 4f core-level spectra ($h\nu = 180$ eV). The change in the CDW-induced core-level splitting is indicated. (c)–(e) Normal-emission Ta 5d and S 3p valence-band spectra as a function of photon energy ($h\nu = 78$–136 eV): (c) off the stripe, (d) on the stripe, and (e) weighted difference between (d) and (c). The solid lines in the left panels of (c) and (d) are guides to the eye highlighting band dispersion. Spectra plotted in the right panels represent spectra averaged over the full photon energy interval. The arrows in (c) mark the energy intervals of the Ta 5d and S 3p states, respectively. In (e) the indicated shift of the leading peak signals the opening of a gap at the Fermi level.

associated with surface Rb ("S") and intercalated Rb ("I") in Figs. 2(h) and 2(i) suggests that most of the deposited Rb atoms are indeed intercalated (if one considers the attenuation of the intercalated Rb signal by the topmost S-Ta-S sandwich).

The link to previous, spatially integrated photoemission results on Rb/1T-TaS_2[22,24] is provided by the ARPES results shown in Fig. 3, which were obtained from a sample on which a Rb stripe similar to the one depicted in Fig. 1(d) had been prepared. Since the width of the stripe roughly matched the diameter of the synchrotron light spot on the sample, it was possible to reveal the Rb-induced changes in the local electronic structure at high spectral resolution by placing the light spot on and off the Rb stripe.

The left column of Fig. 3 shows the adsorbate Rb 3d [Fig. 3(a)] and the substrate Ta 4f [Fig. 3(b)] core-level emissions as measured on and off the stripe. As indicated in Fig. 3(a), the on-stripe Rb 3d spectrum can unambiguously be decomposed into two Doniach-Šunjić-type spin-orbit doublets corresponding to surface Rb and intercalated Rb, where the assignment is corroborated by the relative decrease of the intercalated-Rb component upon going to grazing electron emission angles (spectra not shown). The right column of Fig. 3 displays the on-stripe [Fig. 3(c)] and off-stripe [Fig. 3(d)] substrate valence-band emissions (from Ta 5d and S 3p states) as a function of photon energy, as well as the weighted difference between the two [Fig. 3(e)]. As these series of spectra were recorded in a normal-emission geometry, they directly reflect the band dispersion along the Γ-A symmetry direction, which is perpendicular to the layers [see Fig. 1(b)].

The adsorbate and substrate specific spectral modifications seen on the stripe agree qualitatively and quantitatively with the ones recorded on homogeneously intercalated surfaces:[22,24] (i) The ratio of 0.84 of the integrated Rb 3d signals corresponding to the intercalated and surface species [Fig. 3(a)] indicates that $(75 \pm 5)\%$ of the Rb detected on the stripe is in fact intercalated;[30] (ii) the increase in the Ta 4f core-level splitting from 0.54 eV to 0.73 eV [Fig. 3(b)] signals the transition to the $c(2\sqrt{3} \times 4)$ $rect.$ CDW state; and (iii), in the Ta 5d and S 3p valence-band region, the opening of the 0.39-eV-wide energy gap at the Fermi level and the flattening of the dispersion perpendicular to the layers [Figs. 3(c)–3(e)] are direct evidence for the combined metal-to-insulator and quasi-2D-to-2D transition in the electronic structure. Note that the gap and the flat bands become readily apparent when the remaining contributions from nonintercalated regions are appropriately subtracted from the data taken on the Rb stripe [Fig. 3(e)]. Also note the high sharpness of all the TaS_2 spectral features seen on the Rb stripe, which implies that the initial high crystal quality has been preserved upon intercalation.

IV. CONCLUSION

In summary, our STM, PEEM, and ARPES results on 1T-TaS_2 surfaces that were exposed to focused Rb deposition reveal a clear spatial correlation between adsorbate intercalation and pronounced changes in the structural and electronic properties of the substrate surface. The topmost S-Ta-S sandwich is structurally and electronically decoupled from the bulk, the CDW within the Ta layer is strongly modified, and a distinct metal-to-insulator transition occurs. Since these effects are exclusively observed on intercalated Rb islands, we may conclude that Rb intercalation is their driving force. Our results further demonstrate that the intercalated islands can be sharply confined on the nanometer length scale [Fig. 1(c)], and that larger confined structures consisting of overlapping islands can be created by focused deposition [Fig. 1(d)]. As to the intercalation process, these observations imply that the room-temperature Rb diffusion length in the van der Waals gap of 1T-TaS_2 is rather short, and that the intercalation channels open during deposition at selected points in those areas of the surface that are directly hit by the Rb beam.

Taken together, our results establish focused alkali deposition and intercalation as a tool to tailor the interlayer coupling and electronic properties of layered crystals *in situ* on nanometer- to micrometer-length scales. The tool may prove useful not only in the study of dimensional crossover effects but also in the design of electronic devices based on layered (correlated electron) materials.

[1]A. P. Ramirez, Science **315**, 1377 (2007).
[2]R. Ramesh and D. G. Schlom, MRS Bull. **33**, 1006 (2008).
[3]J. Mannhart and D. G. Schlom, Science **327**, 1607 (2010).
[4]M. Imada, A. Fujimori, and Y. Tokura, Rev. Mod. Phys. **70**, 1039 (1998).
[5]Y. Tokura and N. Nagaosa, Science **288**, 462 (2000).
[6]E. Dagotto, Science **309**, 257 (2005).
[7]H. Takagi and H. Y. Hwang, Science **327**, 1601 (2010).
[8]J. A. Wilson and A. D. Yoffe, Adv. Phys. **18**, 193 (1969).
[9]J. A. Wilson, F. J. Di Salvo, and S. Mahajan, Adv. Phys. **24**, 117 (1975).
[10]K. Rossnagel, J. Phys. Condens. Matter **23**, 213001 (2011).
[11]R. H. Friend and A. D. Yoffe, Adv. Phys. **36**, 1 (1987).
[12]P. Fazekas and E. Tosatti, Philos. Mag. B **39**, 229 (1979).
[13]B. Dardel, M. Grioni, D. Malterre, P. Weibel, Y. Baer, and F. Lévy, Phys. Rev. B **45**, 1462(R) (1992); **46**, 7407 (1992).
[14]K. Rossnagel and N. V. Smith, Phys. Rev. B **73**, 073106 (2006).
[15]B. Sipos, A. F. Kusmartseva, A. Akrap, H. Berger, L. Forró, and E. Tutiš, Nat. Mater. **7**, 960 (2008).
[16]W. B. Clark and P. M. Williams, Philos. Mag. **35**, 883 (1977).
[17]G. J. Tatlock and J. V. Acrivos, Philos. Mag. B **38**, 81 (1978).
[18]C. Pettenkofer, W. Jaegermann, and B. A. Parkinson, Surf. Sci. **251-2**, 583 (1991).
[19]C. Pettenkofer and W. Jaegermann, Phys. Rev. B **50**, 8816 (1994).
[20]R. Adelung, J. Brandt, L. Kipp, and M. Skibowski, Phys. Rev. B **63**, 165327 (2001).
[21]H. J. Crawack and C. Pettenkofer, Solid State Commun. **118**, 325 (2001).
[22]K. Rossnagel, E. Rotenberg, H. Koh, N. V. Smith, and L. Kipp, Phys. Rev. Lett. **95**, 126403 (2005).
[23]P. Schmidt, J. Kröger, B. M. Murphy, and R. Berndt, New J. Phys. **10**, 013022 (2008).
[24]K. Rossnagel, New J. Phys. **12**, 125018 (2010).
[25]F. S. Ohuchi, W. Jaegermann, C. Pettenkofer, and B. A. Parkinson, Langmuir **5**, 439 (1989).
[26]H. I. Starnberg, H. E. Brauer, L. J. Holleboom, and H. P. Hughes, Phys. Rev. Lett. **70**, 3111 (1993).
[27]P. Schmidt, B. Murphy, J. Kröger, H. Jensen, and R. Berndt, Phys. Rev. B **74**, 193407 (2006).
[28]H. J. Crawack, Y. Tomm, and C. Pettenkofer, Surf. Sci. **465**, 301 (2000).
[29]S. E. Stoltz, H. I. Starnberg, and L. J. Holleboom, Phys. Rev. B **67**, 125107 (2003).
[30]We assume an electron inelastic mean free path $\lambda = (5 \pm 0.5)$ Å and that all intercalated Rb atoms are located $d = 6$–7 Å below the surface. Then, if the attenuation of the signal from the intercalated atoms is taken into account via $I(d) = I(0)\exp(-d/\lambda)$, the measured ratio of 0.84 of the Rb $3d$ intensities originating from the intercalated and surface species corresponds to a ratio of the chemical concentrations of 3.25 ± 0.75.